EFDA–JET–PR(10)61

S. Brezinsek, T. Loarer, K. Krieger, S. Jachmich, M. Tsalas, I. Coffey, H.G. Esser, T. Eich,W. Fundamenski, C. Giroud, S. Grünhagen, A. Huber, U. Kruezi, S. Knipe, G.P. Maddison, K. McCormick, A.G. Meigs, Ph. Morgan, V. Philipps, G. Sergienko, R. Stagg, M.F. Stamp, F.L. Tabares and JET EFDA contributors

Fuel Retention in Impurity Seeded Discharges in JET after Be Evaporation

Fuel Retention in Impurity Seeded Discharges in JET after Be Evaporation

S. Brezinsek[1], T. Loarer[2], K. Krieger[3], S. Jachmich[4], M. Tsalas[5], I. Coffey[6], H.G. Esser[1], T. Eich[3],W. Fundamenski[6], C. Giroud[6], S. Grünhagen[6], A. Huber[1], U. Kruezi[1], S. Knipe[6], G.P. Maddison[6], K. McCormick[3], A.G. Meigs[6], Ph. Morgan[6], V. Philipps[1], G. Sergienko[1], R. Stagg[6], M.F. Stamp[6], F.L. Tabares[7] and JET EFDA contributors*

JET-EFDA, Culham Science Centre, OX14 3DB, Abingdon, UK

[1] Institute of Energy and Climate Research - Plasma Physics, Forschungszentrum Jülich, Association EURATOM-FZJ, Partner in the Trilateral Euregio Cluster, Jülich, Germany
[2]CEA, IRFM, F-13108 Saint-Paul-lez-Durance, France
[3]Max-Planck-Institut für Plasmaphysik, EURATOM-IPP, D-85748 Garching, Germany
[4]Association Euratom-Etat Belge, ERM-KMS, Partner in the Trilateral Euregio Cluster, Brussels, Belgium
[5]Association EURATOM-Hellenic Republic, NCSR "Demokritos", Attica, Greece
[6]EURATOM-CCFE Fusion Association, Culham Science Centre, OX14 3DB, Abingdon, OXON, UK
[7]Laboratorio Nacional de Fusión, Asociación EURATOM/CIEMAT, Avenue Complutense 22, 28040 Madrid, Spain
** See annex of F. Romanelli et al, "Overview of JET Results", (23rd IAEA Fusion Energy Conference, Daejon, Republic of Korea (2010)).*

Preprint of Paper to be submitted for publication in
Nuclear Fusion

ABSTRACT.
Preparatory experiments for the ITER-Like Wall in JET were carried out to simulate the massive Be first wall by a thin Be layer, induced by evaporation of about 2.0g Be, and to study its impact on fuel retention and divertor radiation with reduced C content and N seeding. Residual gas analysis reveals a reduction of hydrocarbons by one order of magnitude and of O by a factor 5 in the partial pressure owing to the evaporation. The evolution of wall conditions, impurity fluxes, and divertor radiation have been studied in ELMy H-mode plasmas (B_t = 2.7T, I_p = 2.5MA, P_{aux} = 16MW) whereas a non-seeded reference discharge was executed prior to the evaporation.

The in-situ measured Be flux at the midplane increased by about a factor 40 whereas the C flux decreased by ~50% in the limiter phase of the first discharge with respect to the reference, but erosion of the Be layer and partial coverage with C takes place quickly. To make best use of the protective Be layer, only the first four discharges were employed for a gas balance analysis providing a D retention rate of $1.94\times10^{21}Ds^{-1}$ which is comparable to rates with C walls. But the Be evaporation provides a non-saturated surface with respect to D and short term retention is not negligible in the balance; the measured retention is overestimated with respect to steady-state conditions like for the ILW. Moreover, C was only moderately reduced and co-deposition of fuel with eroded Be and C occurs.

The lower C content leads to a minor reduction in divertor radiation as the reference phase prior to seeding indicates. N adds to the radiation of D and remaining C, and the N content rises due to the legacy effect which has been quantified by gas balance to be 30% of the injected N. C radiation increases with exposures time, and both contributors causing an increase of the radiated fraction in the divertor from 50% to 70%. The radiation pattern suggests that N dominates the increase in the first discharges though C is still the dominating radiator. Therefore, the validity of a proxy of the Be first wall by a thin Be layer is limited and restricted to plasma operation directly after the Be evaporation.

1. INTRODUCTION

ITER will operate in the non-active phase with Plasma-Facing Components (PFCs) made of Be for the main chamber, Carbon-Fibre Composite (CFC) for the divertor target plates, and W for the divertor baffle and dome area. The divertor foreseen for the activated operational phase will be made purely of W. The replacement of CFC by W is governed by the need to remain within the safety limit for the in-vessel tritium inventory, and thus, to minimise the tritium retention which is in carbon-dominated machines determined by co-deposition in layers in remote and partially inaccessible areas. A drawback of the exchange is the loss of intrinsic C radiation in the divertor and the need of extrinsic impurity seeding to achieve a radiating divertor and detached plasma operation which is necessary for divertor integrity. In the ITER-Like Wall (ILW) experiment at JET [1], replacement of PFCs made of CFC by massive Be in the main chamber and W in the divertor will be done, providing an ideal test bed for ITER.

Preparatory experiments for the ILW were conducted with the current PFCs made of CFC aiming on the one hand to document the fuel retention and the material migration to remote areas in reference plasmas, and on the other to develop wall-compatible plasma scenarios with respect to power handling and material erosion [2]. In particular impurity seeding has been identified to be mandatory to assure integrity of the PCFs made of W by sufficient divertor radiation. Plasma scenarios with nitrogen and neon seeding were developed [3] providing compatibility with the envisaged engineering limits for the PFCs, in particular for the outer-target plate [4] and will allow repetition of the discharges with the ILW. However, the total divertor radiation in these experiments represents not solely radiation from the seeding species but always a combination of seeding species and carbon whereas the contribution from the seeding species to the total radiation has been varied extensively [5].

Here, we report on a specific ILW preparatory experiment which was carried out to simulate the massive Be first wall by a thin Be layer, induced by an extended Be evaporation, and to study its impact on fuel retention and divertor radiation with transiently reduced C content [6]. Additionally, impurity seeding with N was applied in order to compensate for the transient loss in C radiation, thus, the experiment is to a certain extend complementary to [5], providing constant extrinsic impurity radiation with increasing C radiation due to re-erosion of the protective Be layer. The Be evaporation executed in this experiment is referred below as extended evaporation due to the fact that 50 times more Be is evaporated with respect to regular performed standard evaporations for conditioning of the JET vessel. Though such an extended Be evaporation [7] provides only a transient and inhomogeneous coverage of the first wall, it can still be seen as a first small step on the way from a CFC to a Be first wall, providing an outlook on what can be expected from the ILW. Moreover, this integrated and ILW-compatible experiment can be re-executed as plasma operation in H-mode resumes and will thereby assess the ILW concerning changes in fuel retention and divertor radiation.

Characterisation of the extended Be evaporation and quantification of the achieved C suppression is described in section 2. The evolution of the wall conditions and the increase of C radiation in time with constant N injection rate have been studied in a series of comparable plasmas in fixed magnetic configurations. The target scenario in standard type I ELMy H-mode was developed in [3] to achieve compatibility with ILW engineering limits. The D_2 fuelling and N2 seeding rate have been chosen deliberately to obtain electron temperatures (T_e) at the outer-target plate which will inhibit physical sputtering and minimise W erosion in the future ILW divertor. The plasma conditions in the core and at the outer target for both parts of the experiment, gas balance analysis and study of the nitrogen contribution to the divertor radiation, are presented in section 3. Section 4 deals with the analysis of the gas balance with the Active Gas Handling System (AGHS) [8] providing a detailed balance of the injected and retained fuel and seeding gas. The variation in the total impurity radiation and the radiation distribution in the divertor with increasing plasma exposure time are discussed in section 5. Finally, conclusions are drawn in section 6 with respect to the extrapolation of results to the ILW.

2. BE EVAPORATION

Four Be evaporator heads were inserted near the vessel midplane and operated at temperatures between 920° and 960°C in vacuum for a cumulated duration of 8 hours per head. In total about 2.0g of Be was evaporated from the four point-like sources equally distributed in toroidal direction. This corresponds to an equivalent Be deposit of about 12nm layer thickness on the first wall though toroidally and poloidally inhomogeneous distributed. The layer thickness was extrapolated from a time-resolved deposition measurement during a Be evaporation with several evaporation cycles at different head temperatures, recorded in-situ by a Quartz Micro-Balance (QMB) positioned on the outer divertor apron. The measured integral frequency increase of 280Hz corresponds to a local deposition of 7×10^{16}Be/cm^2 on the quartz crystal. Considering the ratio of quartz surface to a sphere of 1.5m radius, reflecting the distance between QMB and Be head, one calculates an equivalent amount of 0.5g Be evaporated from the single head in the line-of-side of the QMB. The same amount of Be per head has been evaporated in the integrated experiment with gas balance and impurity seeding discussed here. The deposition of Be into the divertor is limited due to geometrical reasons. Simulation of the poloidal distribution of Be deposited on the first wall and subsequent erosion by plasma impact under different plasma conditions is presented in detail in [9].

A reference discharge prior to the extended Be evaporation discussed here was executed to document the initial influx levels of impurities such as oxygen, hydrocarbons and carbon with optical spectroscopy. Prior to the evaporation a residual gas analysis was performed by a Residual Gas Analyser (RGA) and the gas composition in the vacuum vessel determined. The RGA reference spectrum is depicted in fig. 1a) and shows apart from the dominant deuterium mass substantial contributions of the $C_1(H,D)_x$, $C_2(H,D)_y$ and $C_3(H,D)_z$ group, the cracking pattern of deuterated water as well as contributions from oxygen and carbon mono- and dioxide. The three groups of hydrocarbons are thereby dominated by the deuterated counterparts, e.g. the low contribution of mass 15 with respect to mass 16 indicated practical the absence of CH_4, whereas substantial CD_4, comparable to the contribution of normal and deuterated water, is present though its cracking pattern is partially masked by other species. An RGA scan recorded after execution of the Be evaporation just prior to the first plasma is depicted in fig. 1, too.

A substantial reduction of all groups of deuterated hydrocarbons by about one order of magnitude in the partial pressure after applying the evaporation is detectable revealing a significant coverage of the CFC and carbon layer surfaces with Be. Moreover, the getter of oxygen can additionally be observed by a further reduction of the corresponding masses 32 and 16, partially masked by hydrocarbons, of about a factor 5. Less reduction is detected for mass 40, representing mainly Ar, which remains almost unaffected in the residual gas in the vessel, probably due to poor pumping of the species.

Figure 2 shows the impact of the extended Be evaporation on the erosion of the first wall measured by optical spectroscopy at one of the inner poloidal limiter. Details about the spectroscopic system and the line-of-sight at the vessel midplane are described in [7]. All photon fluxes have the same scale

for a relative comparison of the source strength and coverage of Be and C, measured by the localised impurity flux of Be+ and C+ ions which results from sputtering by mainly impinging deuterium ions and CXRS neutrals. However, the Be fluxes represent an unresolved folding of erosion of the thin Be layer as well as include the surface coverage of the limiter with the Be coating. The limiter phase with contact at the inner wall limiter was minimised to 3s in all discharges (t = 1.5-4.5s) to avoid too strong sputtering due to the high temperature edge plasma. The upper part of fig. 2 refers to integral measurements in this time frame whereas the lower part refers to a time period in the divertor phase (t = 19.0-22.0s) with additional heating as discussed in the next section.

The success of the enhanced Be evaporation with respect to first wall Be coating coverage can be seen by comparison of the C and Be erosion fluxes in the limiter phase of the first discharge after the Be evaporation with the reference beforehand. The Be erosion flux measured by BeII at 436.0nm at the midplane was increased by about a factor 40 (fig.2a) whereas the corresponding C flux, measured by CII at 426.7nm, decreased only by ~50% in with respect to the reference discharge (fig.2(b)). The transient coating of the first wall by evaporated Be was with respect to significant suppression of C erosion successful. However, strong erosion of the Be layer and partial deposition of the limiter by C occurs on a short timescale, and already in the first 4 discharges (~120 plasma seconds), which have been used for the gas balance study, already the Be flux in the limiter phase is decreased to 25% of the initial value of the first discharge as depicted in fig.2a). The absolute value lays thereby about one order above the reference prior to the evaporation. The C erosion flux (fig.2b) increases in the same manner quickly to about 60% of the reference value and remains at this level.

The opposing trend of the Be and C erosion flux evolution with discharge time is even more pronounced in the divertor phase as it is shown in fig.2c) and 2d). Both fluxes show that in the divertor phase with an inner wall clearance of 10cm already the impact of the Be evaporation is halfway gone: BeII is decreased to half the initial flux and CII is increased to half the initial flux of the first discharge. Overall both phases, the short limiter phase as well as the long divertor phase, contribute significantly to the re-erosion of the protective Be layer. Due to the transient behaviour only these first four discharges were applied later for analysis of the wall inventory. However, the decay of the Be flux in the divertor phase in time is faster than in previous experiments with extended Be evaporation in L-mode plasmas without limiter phase and larger wall clearance [7]. The higher Be erosion flux in the divertor phase may be attributed to a stronger wall interaction during ELM burst in the applied H-mode plasmas in comparison to L-mode plasmas studied before.

3. PLASMA SCENARIO AND OUTER TARGET PLASMA CONDITIONS

The chosen target scenario for the experiment was a standard fuelled ELMy H-mode ($B_t = 2.7T$, $I_p = 2.5MA$, $q_{95} \sim 3.5$, $P_{aux} = 16MW$, $\delta \sim 0.4$, $f_{gw} \sim 0.95$, $\Delta W_{ELM} \sim 100kJ$) which has been developed in [3]. The D_2 injection ($\Gamma_{D2} = 1.85 \times 10^{22}$e/s) and N_2 injection rate ($\Gamma_{N2} = 3.55 \times 10^{22}$e/s) into the divertor, performed through a ring of toroidally homogenous distributed gas inlets, were chosen deliberately to achieve peak Te at the outer strike point below 10eV which will minimise the W sputtering in

the divertor of the ILW by all remaining impurities (C, N, O etc.). In fact the fuelling rate was even slightly raised with respect to the reference value to achieve the requested high recycling/partial detachment regime at the outer target in order to compensate for expected changes in the fuelling by wall recycling. However, the recycling flux at the outer target plate is by one order higher than the injected deuterium flux and the divertor plasma enters the high recycling or partial detachment regime as discussed below. Figure 3 shows time traces for a number of global parameters such as the deuterium recycling flux in the outer leg given by the D_α photon flux the N_2 seeding rate with injection into the outer Scrape-Off Layer (SOL), the density normalised to the Greenwald density as well as the total input power, the radiated power and the confinement factor. A short phase prior to the nitrogen seeding has been used to follow up the N content in the wall from discharge to discharge. The first four discharges, used for the gas balance studies, are depicted in fig.3a).

Though the waveform and the strength of the seeding is kept constant, the nitrogen inventory increases in time and lead to a transition from type I ELMy H-mode to type III ELMy Hmode with degradation of the confinement in the last discharge from initially $H_{98y} = 0.92$ to 0.83 at $t = 20s$; the non-seeded but deuterium fuelled reference discharge reached $H_{98y} = 0.95$ in the flattop phase. The initial nitrogen recycling flux at the beginning of the first discharge would represent a good compromise with respect to acceptable target conditions and global confinement, however, real-time control on the seeding species N, which would be required to maintain the nitrogen recycling level, has not yet been developed but will be in place with the ILW and account for the nitrogen legacy. The target conditions have been analysed with the aid of a set of Langmuir probes embedded in the outer target plate as well as visible and ultra-violet spectroscopy similar to ones used for analysis in [11]. In fig. 4 are the outer strike-line, the position of the flush-mounted Langmuir probe array (KY4D) and the lines-of-sight of the applied divertor spectroscopy (KT3) depicted. GIM9 is the toroidally symmetric gas injection ring for nitrogen seeding in the SOL.

The applied combination of seeding and fuelling leads to detachment at the outer target associated to peak electron temperature values in-between ELMs below 10eV in the first four discharges as required from the scenario. However, the nitrogen legacy, discussed in detail below, leads to an increase of plasma cooling from discharge to discharge and, thus, to an increase of the degree of detachment and decrease of local Te.

Figure 5 shows the electron temperature and density profiles for the last (JET Pulse No: 78785) of the first four discharges used for the gas balance in comparison with a non-seeded reference (JET Pulse No: 78787) which has been executed as fifth discharge directly after the gas balance experiment under otherwise identical plasma scenario. The electron density and temperature profiles were recorded during a small strike-point sweep at the end of the discharge flattop ($t = 21 - 22s$). For comparison also profiles for the subsequent discharge with N2 injection into the outer SOL (JET Pulse No: 78787) instead of the Private-Flux Region (PFR) (JET Pulse No: 78785) is plotted.

The corresponding core parameters are shown in fig.3b). N2 seeding into the SOL is not inducing type III ELMy H-mode as the seeding into the PFR does under otherwise comparable injection

rates. Moreover, the confinement remains unaffected with the seeding into the PFR which can be seen in comparison with the non-seeded reference discharge (JET Pulse No: 78786), however, the comparison is to a certain extent affected by the nitrogen legacy.

Both discharges with active seeding in either PFR or SOL are partially detached at the outer strike-point with T_e <10eV whereas the discharge without active seeding, but remaining and declining N legacy is reaching a peak T_e ~50eV at the strike point – a typical value for attached H-mode plasmas at the outer target of JET. The peak electron density in the non-seeded reference case reaches $2\times10^{20}m^{-3}$ and drops in the detached cases to $4\times10^{19}m^{-3}$ (seeding into SOL) and $2\times10^{19}m^{-3}$ (seeding into PFR) reflecting a roll over in the ion flux to the target. The flatten profiles in both seeded cases show the extension of the detachment at the outer target plate into the SOL, thereby the seeding into the PFR seems to be more pronounced with a higher degree of detachment. The spectroscopic analysis of Balmer-line widths in the detached case suggests higher electron densities in the divertor in the order of a few $10^{20}m^{-3}$ which are in-line with the appearance of high-n lines and volume recombination in front of the target and electron temperatures of below 5eV.

4. GAS BALANCE ANALYSIS AND NITROGEN LEGACY

In order to have the major benefit of the transient carbon reduction and to make use of the protective Be layer, only the first four successful plasma discharges have been used to perform a gas balance analysis of the fuel and the nitrogen inventory with the aid of the AGHS. Though the very first discharge after the Be evaporation was successfully performed, a number of subsequent discharges had no successful breakdown which is likely related to the purity of the plasma and the high fuel uptake of fresh Be wall. However, the unsuccessful breakdowns are assumed not to influence the gas balance analysis which has been performed in the following way: a cryogenic pump regeneration before and after the four successful discharges has been applied in order to recover the injected gas from only this experiment and analyse it according its composition. The method and precision of the system is described in detail in [8]. The total amount of injected gas is equivalent to 20.6barl D_2 and 2.5barl N_2 whereas 17.3barl have been recovered after 30 minutes. The major fraction of the recovered gas is deuterium (~95%) which leads to a retention rate of $1.94\times10^{21}Ds^{-1}$ related to the accumulated time in divertor configuration of 96s. The retention rate is comparable to retention rates in experiments in pure carbon environment with similar magnetic configuration but at lower electron density [8]. But the measured retention rate in this experiment is overestimated in comparison with the pure carbon references due to the fact that the Be evaporation provides a non-saturated Be-wall surface with respect to deuterium and represents therefore not a steady-state result but includes the short term retention until wall saturation takes place. Indeed the requested gas amount to achieve a similar density in the limiter phase as in CFC is higher in the first pulse after the Be evaporation ($7.5\times10^{21}D$), but equilibrates in the subsequent discharges slowly to the reference value with PFCs made of CFC. Nevertheless also a change of the ratio of the short term

(implantation) and long term (co-deposition) retention is likely and will be also present with the ILW. Indeed after the initial restart phase of the ILW comparative studies will start with saturated Be walls and will not be affected by the transient effect introduced by the fresh wall.

However, the basic mechanism for the relative high fuel retention observed in this experiment is still the co-deposition of deuterium in layers. This is in line with the measured high Be influx from the main chamber into the inner divertor leg which is a net deposition zone for both Be and C. Therefore, the co-deposition occurs to a large extent with freshly eroded Be from the main chamber wall which migrates to the divertor by SOL flows and finally deposits.

Secondly, C was in this experiment only moderately reduced by the inhomogeneous coverage with Be owing to only four evaporator heads and co-deposition with both Be and C takes place. The fraction of co-deposition due to C increases in time when the C source grows due to re-erosion of the protecting Be layer. With the ILW and PFCs made of bulk Be and thick Be coatings these transient effects observed here, wall loading and re-appearance of C, will not happen. Co-deposition of fuel with Be will remain as dominant mechanism for the fuel retention, though we assume that a final transport in remote areas will be reduced with respect to C due to the absence of chemical sputtering for Be and therefore less steps of re-erosion and deposition will occur. Moreover, laboratory experiments [10] suggest less tritium content in Be layers and recovery at lower surface temperatures than for C layers.

In addition to the balance for fuel, also the first gas balance for injected, recovered and retained nitrogen has been performed in JET. About 3.0% of the total gas recovered consists of the seeding and non-recycling impurity N_2. The recovered amount is equivalent to 30% of the injected N_2. The observation is in line with the so-called legacy effect of N which has been observed earlier in JET. Potential explanation for these long last in the vessel is surface dilution of the PFC material by nitrogen leading either to N-containing layers or even to nitride formation as revealed recently for comparable plasmas by spectroscopy in the JET divertor [11]. A similar effect has also been observed in W PFCs in the full W ASDEX-Upgrade [12] and in limiter experiments in TEXTOR [13].

Apart from the gas balance analysis of fuel and seeding gas, the nitrogen legacy has been observed in this experiment in-situ also during plasma discharges by optical spectroscopy and by RGA spectra. Fig.6a) shows three comparative RGA spectra before the Be evaporation, after the N injection of the first four discharges and, finally, after execution of a conditioning discharge with extensive strike-point sweeping aiming in a release of incorporated nitrogen in the vessel. The corresponding difference spectra with respect to the initial RGA reference spectrum before the Be evaporation are depicted in 6(b). The conditioning discharge is similar to the reference discharge apart from the fact that higher hydrocarbons are still below the initial value and methane is significantly increased. Thus, the impact of the extended Be evaporation on the surface coverage of CFC and carbon layers is almost gone after one day of operation.

The second spectra shown in 6(b) provides also indications for remaining nitrogen and the appearance of nitrogen derivates, in particular of deuterated ammonia, in the residual gas prior to

the cryogenic pump regeneration. But there is no indication for the appearance of HCN or DCN though visible spectroscopy clearly identifies in the plasma the production and existence of the CN radical. However, further detailed analysis and simulations are necessary to fully deconvolute the complex cracking pattern of the different species.

Divertor spectroscopy confirms the nitrogen legacy by the prolonged appearance of a nitrogen source over several discharges without active nitrogen seeding – measured in-situ by NII lines. The spectra were taken with the direct imaging spectrometer system (KT3) observing the outer target plate; technical details are described in [11]. Figure 7a) shows the evolution of CII (427.6nm), NII (438.0nm) and BeII (436.0nm) on a discharge to discharge base, whereas the initial values from the reference discharge (#0) and the first discharge without nitrogen seeding (#5) are indicated for t = 18s of each discharge. The operation with detached outer divertor target leads to a reduced C and Be sputtering owing to the lower energy of the impinging ions due to plasma cooling and dilution of the layer surface with impinging nitrogen. These two mechanisms have been identified in the case of carbon layers for different ratios of N to D injection [11], but the observation can likely be extended to Be-containing layers. The sputtering of Be and C increases drastically as indicated by the corresponding photon fluxes when the active seeding is stopped. Though only bare photon fluxes are shown, the conversion to particle fluxes for BeII, CII and D_α with the aid of inverse photon efficiencies (S/XB values) for the different transitions would even strengthen the observation owing to the fact that the S/XB values increase with higher T_e. However, the averaging of the spectroscopic data over ELMs made the quantification of particle fluxes challenging and further analysis is required. Moreover, S/XB values for NII at 438.0nm are unknown for the given divertor conditions.

Figure 7b) shows the spatially resolved time evolution of CII (426.7nm) and NII (438.0nm) recorded in the first discharge without nitrogen seeding - directly after the gas balance was performed. Though interfered by ELMs a clear increase of the averaged CII photon flux with decreasing NII photon flux can be observed. NII reduces to about half of the initial value in the discharge with moderate increase in the local T_e as confirmed by Langmuir probes. The later fact allows the conclusion that the N source is also dropping to half the initial value.

Also the increase in CII emission is related to an increase of the C source owing to the reerosion of the nitrogen-containing layer and the increase of local T_e. In parallel the appearance of CN - the CN B-X has been previously identified in JET [11] - reflects the sputtering of a nitrogen-containing layer in the SOL. The time evolution of the BeII emission at 436.0nm is comparable with the CII emission, indicating that still some Be is on the outer target deposited. However, the nitrogen spectroscopy on NII in the divertor indicated a typical nitrogen legacy of max. 20% which cannot account for the missing amount of nitrogen measured by analysis of the exhausted gas.

5. DIVERTOR RADIATION

The reduction of carbon after the Be evaporation shall have an impact on the radiation in the

divertor. However, the radiation in the reference experimental phase prior to the first nitrogen injection decreased only moderate. Radiation of N adds to the radiation of D and remaining C in the divertor as it can be seen in fig.8(a)-(c) which shows the increase in the radiated fraction in the first discharge after the Be evaporation from $f_{rad} = 30\%$ prior to the seeding, to $f_{rad} = 40\%$ starting with the seeding, and with constant seeding rate into the PFR to $f_{rad} = 50\%$ at the end of the plasma flattop. The bolometric reconstruction in the divertor provides also information about the radiation pattern in-between ELMs and reveals that N, which is injected into the PFR, is mainly radiating close to the x-point whereas C radiates also along the separatrix – as observed elsewhere [12].

In the subsequent discharges the nitrogen content in the divertor increases due to the legacy effect. Also the carbon radiation, mainly C^{3+} and C^{4+} in the divertor starts to increase from discharge to discharge due to erosion of the protective layer in the main chamber and flow of C into the divertor, and both contributors causing an increase of the radiation fraction from initially 50%, at the end of the first pulse, to 60% at the end of the fourth pulse (fig.8(d)) and, finally, to 70% at the end of the experiment (~10th discharge). It is not directly possible to draw firm conclusions about to say which one of the two contributors causes the increase, but the radiation pattern in fig. 8 indicates that the rise in radiation is due to the N increase in time in the first four discharges.

SUMMARY AND CONCLUSION

The transient phase with reduced carbon radiation after extended beryllium evaporation was applied to mimic the ITER-like Wall at JET and to perform a gas balance analysis of the injected fuel under ILW-compatible plasma conditions. Radiating divertor plasmas with detached outer-strike point on the load-bearing plate, which will be with ILW made by bulk tungsten, were executed with nitrogen seeding in order to reduce the power load and to cool down the divertor plasma below 10eV and ensure low sputtering in-between ELMs. The plasma performance is modestly reduced with respect to fuelled type I ELMy H-modes, but fully compatible with the ILW engineering requirements whereas substantial nitrogen legacy has been quantified by the gas balance analysis. The cause and strength of nitrogen legacy in the Be and W environment will become an important subject for the qualification of nitrogen as seeding gas in comparison with other candidates such as noble gases Ne or Ar.

The gas balance, which was performed in the first four discharges after the evaporation, provides a similar fuel retention rate in comparison with comparable plasmas in the CFC environment but without seeding. A reduction of deuterium retention rate as it is expected in the future from the ILW could not be observed in the case of the extended Be evaporation and two reasons have been identified: the short term retention is included in the retention rate as the wall is non-saturated with respect to deuterium and, secondly, the beryllium coverage is incomplete and causes a fast reappearance of carbon in the plasma, as documented by optical emission spectroscopy, and subsequent co-deposition of fuel by Be and C.

However, the compatibility of H-mode plasmas with transiently reduced carbon content has been

demonstrated and initial information about required fuelling rates for the deuterium recycling and the impurity seeding with nitrogen have been obtained. Reference values for fuel retention rates and intrinsic impurity fluxes are recorded and will be compared with plasmas with the ITER-Like Wall at JET as soon as impurity seeding will be required to satisfy the strict divertor power and energy loads and W erosion and concentration requirements.

ACKNOWLEDGEMENTS

This work, supported by the European Communities under the contract of Association between EURATOM and FZJ, was carried out within the framework of the European Fusion Development Agreement. The views and opinions expressed herein do not necessarily reflect those of the European Commission.

REFERENCES

[1]. Matthews G.F. et al 2009 Physica Scripta T**138** 014030
[2]. Brezinsek S. et al 2010 Journal of Nuclear Materials *doi:10.1016/j.jnucmat.2010.10.037*
[3]. Maddison G.P. et al 2010 Journal of Nuclear Materials *doi:10.1016/j.jnucmat.2010.08.059*
[4]. Riccardo V. et al 2009 Physica Scripta T**138** 014033
[5]. Giroud C. et al. in Fusion Energy 2010 (Proc. 23th Int. Conf. Dajeon, 2010) (Vienna: IAEA) CD-ROM file EXC/P3-02 and *http://www-naweb.iaea.org/napc/physics/FEC/FEC2010/html/index.htm*
[6]. Brezinsek S. et al. in Fusion Energy 2010 (Proc. 23rd Int. Conf. Daejeon, 2010) (Vienna: IAEA) CD-ROM file EXD/P3-04 and *http://www-naweb.iaea.org/napc/physics/FEC/FEC2010/html/index.htm*
[7]. Krieger K. et al 2009 Journal of Nuclear Materials **390-391** 110
[8]. Loarer T. et al 2009 Journal of Nuclear Materials **390-391** 20
[9]. Krieger K. et al. in Fusion Energy 2010 (Proc. 23rd Int. Conf. Daejeon, 2010) (Vienna: IAEA) CD-ROM file EXD/P3-19 and *http://www-naweb.iaea.org/napc/physics/FEC/FEC2010/html/index.htm*
[10]. Sugiyama K. et al 2010 Journal of Nuclear Materials *doi:10.1016/j.jnucmat.2010.09.043*
[11]. Brezinsek S. et al 2010 Journal of Nuclear Materials *doi:10.1016/j.jnucmat.2010.12.097*
[12]. Kallenbach A. et al 2010 Journal of Nuclear Materials *doi:10.1016/j.jnucmat.2010.11.105*
[13]. Rubel M. et al 2010 Journal of Nuclear Materials *doi:10.1016/j.jnucmat.2010.08.035*

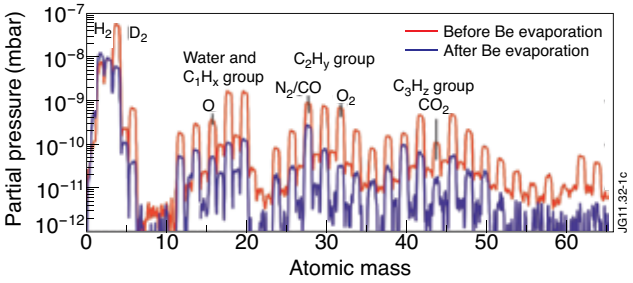

Figure 1: RGA spectrum prior and post the extended Be evaporation. Strong reduction of hydrocarbons (H stands for the isotopes H or D), water, and oxygen can be detected after the evaporation.

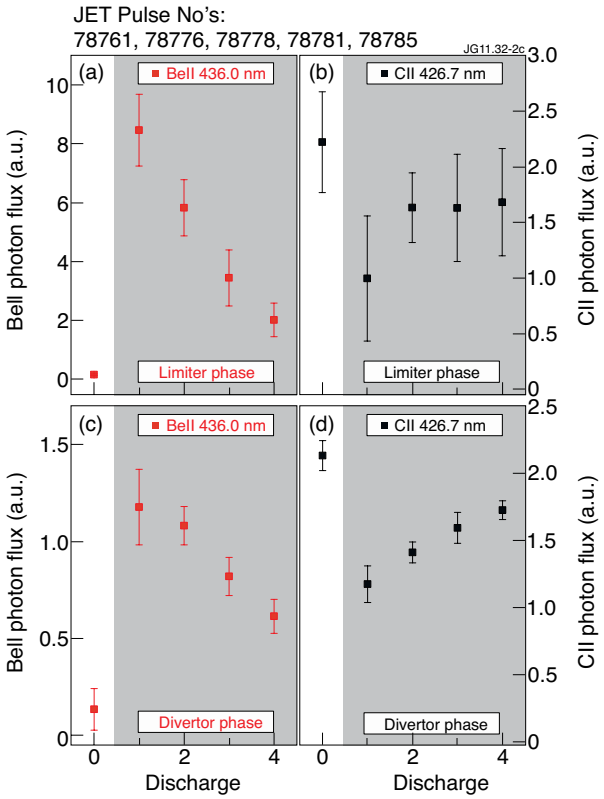

Figure 2: Optical emission spectroscopy observing an inner poloidal limiter at the midplane. The reference discharge prior to the extended Be evaporation is labeled as discharge 0. (a) Discharge-to-discharge development of BeII (436.0nm) emission averaged during the limiter phase. (b) Corresponding CII (426.7nm) emission during the limiter phase. (c) Discharge-todischarge development of BeII (436.0nm) emission averaged during the divertor phase (t = 19- 22s). (d) Corresponding CII (426.7nm) emission during the divertor phase.

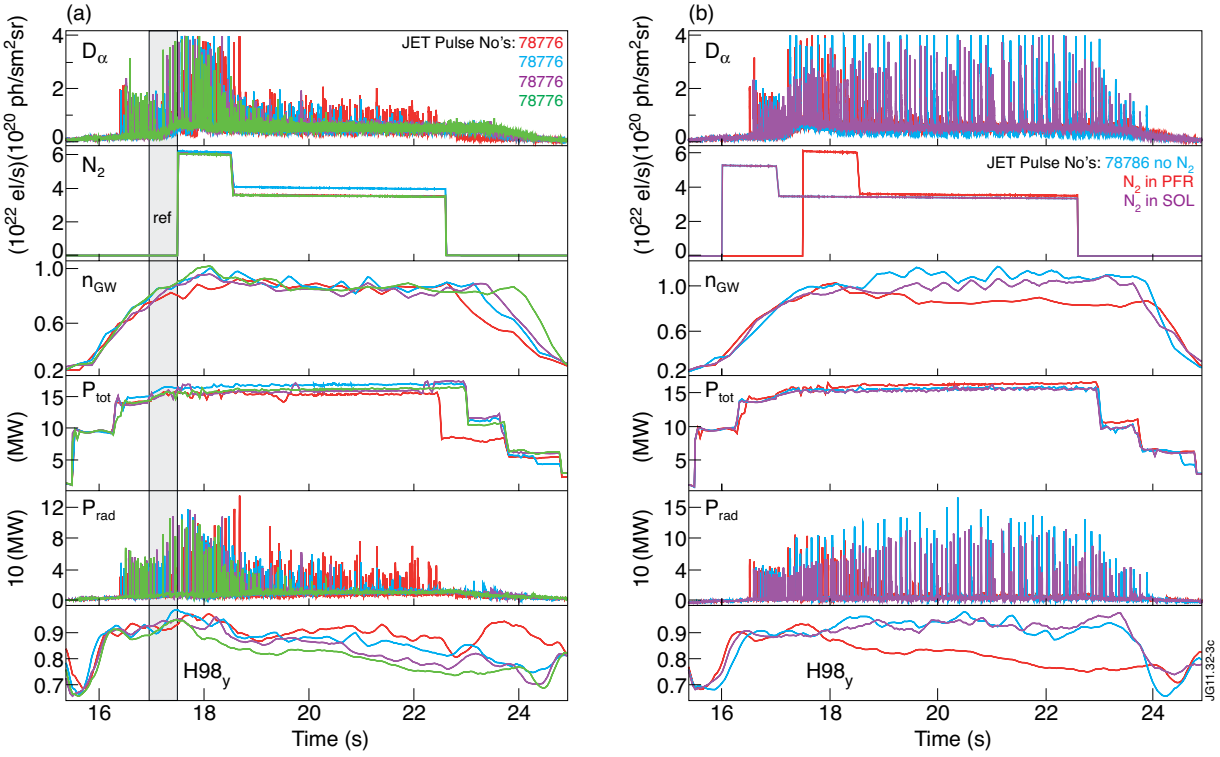

Figure 3: Time traces of characteristic plasma properties: deuterium flux, seeding rate, Greenwald fraction, input power, radiate power, and confinement factor. (a) The first four discharges used for the gas balance analysis. Nitrogen tends to build up a legacy in the vessel which leads finally to degradation of the confinement in time at constant seeding rate. (b) Comparison of discharges with N_2 injection into the SOL (JET Pulse No: 78787), N_2 injection into the PFR (JET Pulse No: 78785), and a reference discharge without active seeding (JET Pulse No: 78786).

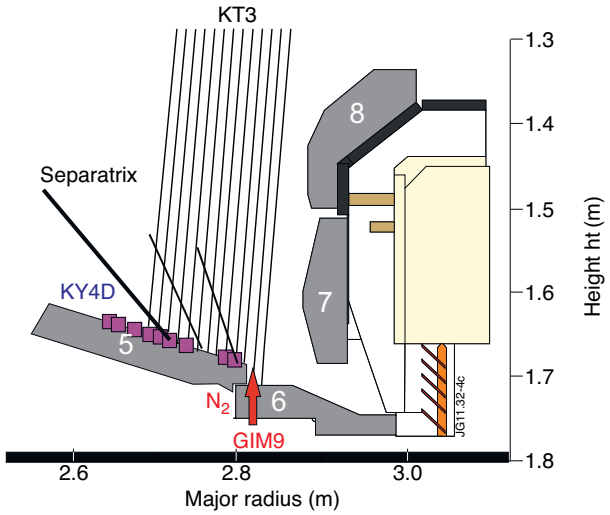

Figure 4: Lines-of-sight of the divertor spectroscopic system (KT3) in this experiment and position of Langmuir probes (KY4D) embedded in the target plate of the outer divertor leg. The separatrix as well as the location of the nitrogen injection ring (GIM9) are indicated.

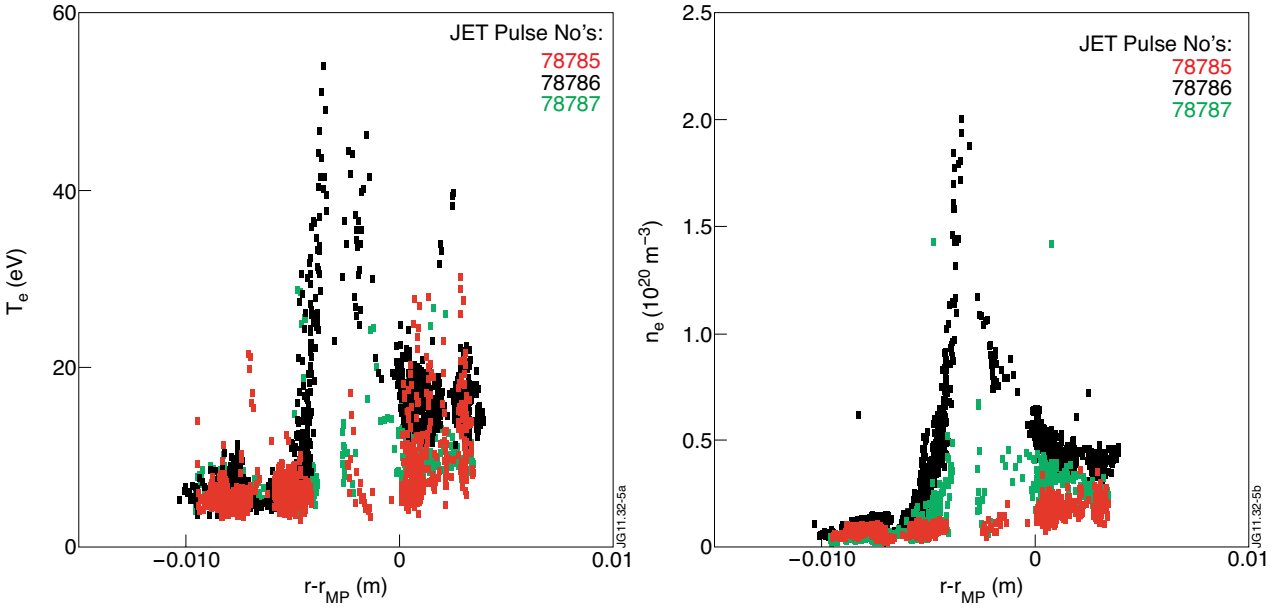

Figure 5: Electron temperature profile (left) and electron density profile (right) at the outer target plate in discharges with N_2 seeding into the outer SOL (JET Pulse No: 78785), into the PFR (JET Pulse No: 78787) and without active seeding (JET Pulse No: 78786). The non-seeded discharge was executed between the other two cases. The profiles are mapped to the outer midplane.

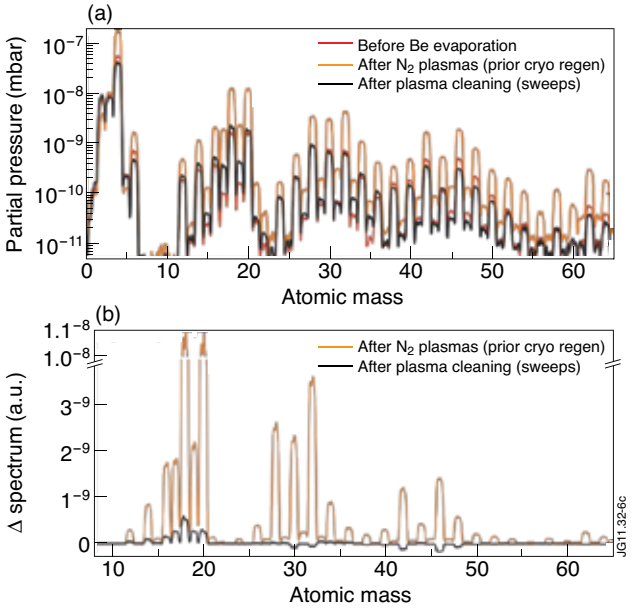

Figure 6: (a) Comparison of RGA spectra taken after a reference discharge, after four consecutive plasma discharges with nitrogen seeding and after a cleaning discharge without seeding but with strike-point sweeping. (b) Corresponding difference spectra which show that the cleaning discharges were successful, but also the impact of the Be evaporation on wall conditions is almost gone.

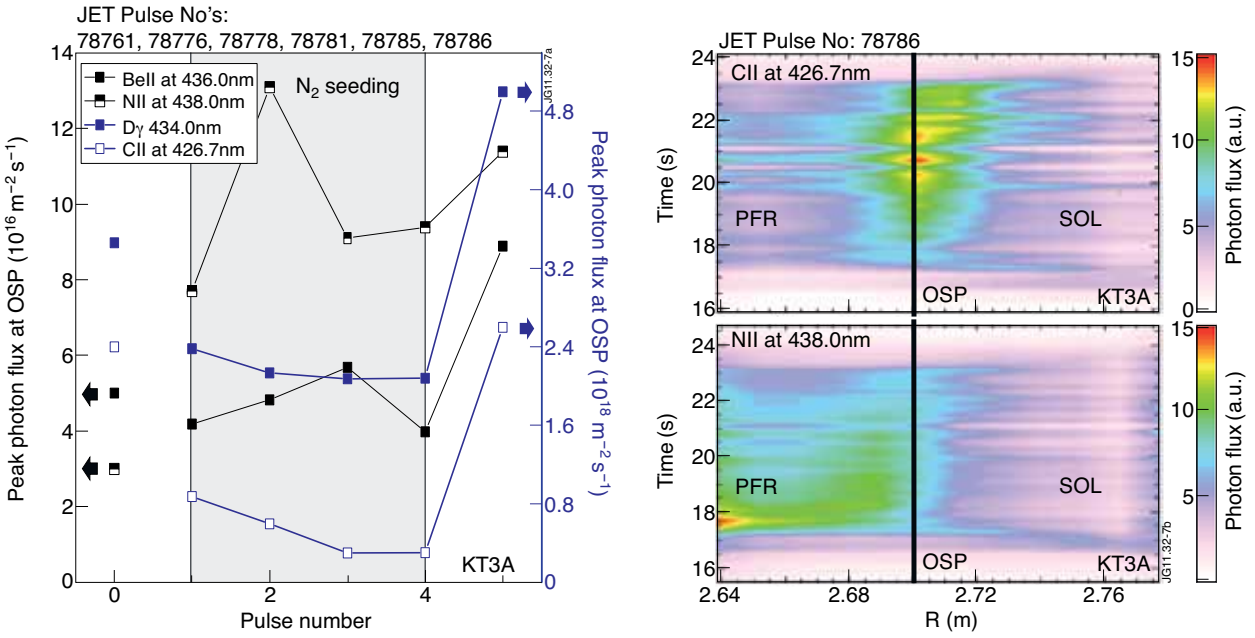

Figure 7: (a) Discharge-to-discharge evolution of CII (426.7nm), NII (438.0nm) and BeII (436.0nm) at t = 18s. The indicated reference values are taken from the discharge before the Be evaporation (JET Pulse No: 78761). (b) Temporal evolution of NII and CII emission in the first discharge without active nitrogen seeding. CII reappears quickly as NII reduces in time.

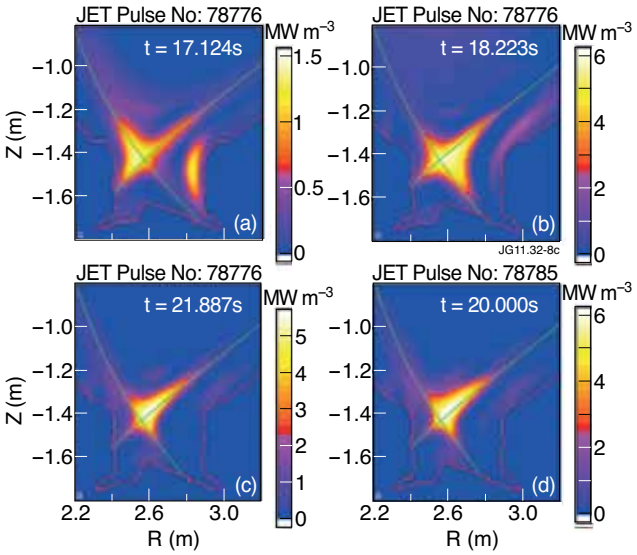

Figure 8: Divertor radiation distribution in the first discharge after the Be evaporation (JET Pulse No: 78776): the radiation pattern (a) prior to N_2 injection (f_{rad} = 30%), (b) with start of N_2 injection (f_{rad} = 40%), and (c) after 2.5s of N_2 injection (f_{rad} = 50%). For comparison the radiation pattern in the fourth plasma discharge after the Be evaporation (JET Pulse No: 78785) is shown in (d); frad increases to 60% though the N_2 injection rate remains constant.